

*Rapid Note***Magnetic field induced phase transitions in  $\text{YBa}_2\text{Cu}_4\text{O}_8$** T. Schneider<sup>a</sup> and J.M. Singer

Physikinstitut, Universität Zürich, Winterthurerstrasse 190, 8057 Zürich, Switzerland

Received 21 December 1998 and Received in final form 3 February 1999

**Abstract.** The  $c$ -axis resistivity measurements in  $\text{YBa}_2\text{Cu}_4\text{O}_8$  from Hussey *et al.* for magnetic field orientations along the  $c$ -axis as well as within the  $ab$ -plane are analyzed and interpreted using the scaling theory for static and dynamic classical critical phenomena. We identify a superconductor to normal conductor transition for both field orientations as well as a normal conductor to insulator transition at a critical field  $H_c \parallel a$  with dynamical critical exponent  $z = 1$ , leading to a multicritical point where superconducting, normal conducting and insulating phases coexist.

**PACS.** 74.25.Dw Superconductivity phase diagrams – 74.25.Fy Transport properties (electric and thermal conductivity, thermoelectric effects, etc.)

Recently it has been demonstrated, that the doping tuned superconductor to insulator (SI) transition in cuprates can be understood in terms of quantum critical phenomena in two dimensions [1,2]. Zero temperature magnetic field driven SI transitions have also been observed in ultrathin Bi films, and successfully interpreted in terms of the scaling theory of quantum critical phenomena [3]. Nevertheless, three important questions concerning the physics of insulating and superconducting cuprates remain open. One is the nature and dimensionality of the normal state revealed when superconductivity is suppressed by a magnetic field [4–7] and the second is the role of disorder. The third issue concerns the dynamical universality classes of SI and superconductor to normal state (SN) transitions at finite temperatures.

We address these three issues through an analysis and interpretation of recent out-of-plane resistivity measurements  $\rho_c$  of  $\text{YBa}_2\text{Cu}_4\text{O}_8$  in magnetic fields by Hussey *et al.* [7], using the scaling theory of static and dynamic classical critical phenomena. Since this material is stoichiometric and, therefore, can be synthesized with negligible disorder, we consider the pure case. As shown below, the experimental data for  $\rho_c(T, \mathbf{H} \parallel c)$  are consistent with a magnetic field tuned SN transition, while the data for  $\rho_c(T, \mathbf{H} \parallel a)$  provide strong evidence for a multicritical point at the critical field,  $\mathbf{H}_{cr} \parallel (a, b)$ , where the superconducting, normal conducting and insulating phases coexist. Moreover, from the existence of a critical resistivity,  $\rho_{c,cr}$  for  $\mathbf{H} \parallel a$ , where the magnetic field tuned multicritical point occurs, we derive its dynamical universality class,  $z = 1$ , uniquely. For general magnetic field orientations,

we predict a line of multicritical points provided that the critical resistivity  $\rho_{c,cr}$  is attainable.

The appropriate approach to uncover the phase diagram from conductivity measurements is the scaling theory of classical dynamic critical phenomena [8]. We now sketch the essential predictions of this theory in terms of a dimensional analysis. A defining characteristic of a superconductor is its broken U(1) or gauge symmetry, which is reflected in the order parameter  $\Psi$ . Gauge invariance then implies the following identification for the gradient operator

$$i\nabla\Psi \longrightarrow i\nabla\Psi + \frac{2\pi}{\Phi_0}\mathbf{A}. \quad (1)$$

The basic scaling argument, which amounts to a dimensional analysis, states that the two terms on the right hand side must have the same scaling dimension,  $(\text{Length})^{-1} \equiv L^{-1}$ . The dimensionality of the magnetic and electric field are then expressed as

$$\mathbf{H} = \nabla \times \mathbf{A} \propto L^{-2}, \quad \mathbf{E} = -\frac{1}{c} \frac{\partial \mathbf{A}}{\partial t} \propto (Lt)^{-1}. \quad (2)$$

In a superconductor the order parameter  $\Psi$  is a complex scalar,

$$\Psi = \text{Re}(\Psi) + i\text{Im}(\Psi),$$

corresponding to a vector with two components. Consequently, the dimensionality of the order parameter is  $n = 2$ . Based upon the dimensional statement

$$\xi = \xi_0^\pm |\epsilon|^{-\nu} \propto L, \quad \epsilon = \frac{T - T_c}{T_c}, \quad (3)$$

---

<sup>a</sup> e-mail: jms@physik.unizh.ch

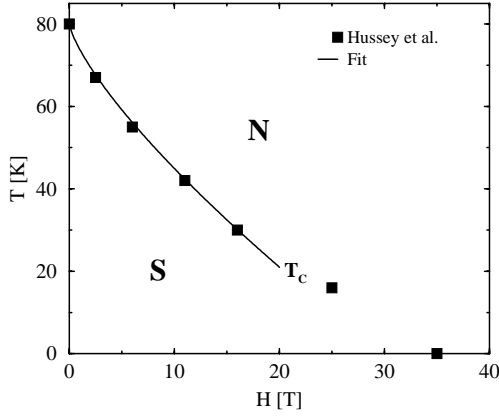


**Fig. 1.**  $T$ - $H$ -phase diagram for Y-124,  $\mathbf{H} \parallel c$ . The data points  $T_c$  vs.  $H_c$  have been deduced from [7]. The solid curve corresponds to the limiting behavior given by equation (15).

where  $\pm = \text{sign}(\epsilon)$ , we obtain in  $D$  dimensions for the free energy density the scaling form

$$f = F/(Vk_B T) \propto L^{-D} \propto (\xi^\pm)^{-D}, \quad (4)$$

and for  $\mathbf{H} \neq 0$

$$f = (\xi^\pm)^{-D} \mathcal{G}(\mathcal{Z}), \quad \mathcal{Z} = \frac{H(\xi^\pm)^2}{\Phi_0}, \quad (5)$$

due to equation (2).  $\mathcal{G}$  is an universal scaling function of its argument  $\mathcal{Z}$ . An extension to 3D anisotropic materials, such as cuprates, is straightforward [9]:

$$f = (\xi_x^\pm \xi_y^\pm \xi_z^\pm)^{-1} \mathcal{G}(\mathcal{Z}), \quad (6)$$

where the indices  $x, y, z$  denote the corresponding crystallographic  $b, a, c$ -axes of the cuprates, and

$$\begin{aligned} \mathbf{H} = H(0, \sin \delta, \cos \delta): \\ \mathcal{Z} &= \frac{(\xi_x^\pm)^2}{\Phi_0} \sqrt{\left(\frac{\xi_z}{\xi_x}\right)^2 H_y^2 + \left(\frac{\xi_y}{\xi_x}\right)^2 H_z^2}, \\ \mathbf{H} = H(\cos \phi, \sin \phi, 0): \\ \mathcal{Z} &= \frac{(\xi_z^\pm)^2}{\Phi_0} \sqrt{\left(\frac{\xi_y}{\xi_z}\right)^2 H_x^2 + \left(\frac{\xi_x}{\xi_z}\right)^2 H_y^2}. \end{aligned} \quad (7)$$

Using this scaling form of the free energy density magnetization [10,11] and magnetic torque data [9,12] have been successfully analyzed.

Of particular interest in the present context is the conductivity  $\sigma$ . From the dimension of the current,

$$\mathbf{J} = \frac{1}{c} \frac{\partial f}{\partial \mathbf{A}} \propto L^{-D+1}, \quad (8)$$

and the electric field (see Eq. (2)), we obtain for the electric conductivity

$$\sigma = \frac{J}{E} \propto tL^{2-D} \propto \xi^{2-D+z}, \quad t \propto \xi^z, \quad (9)$$

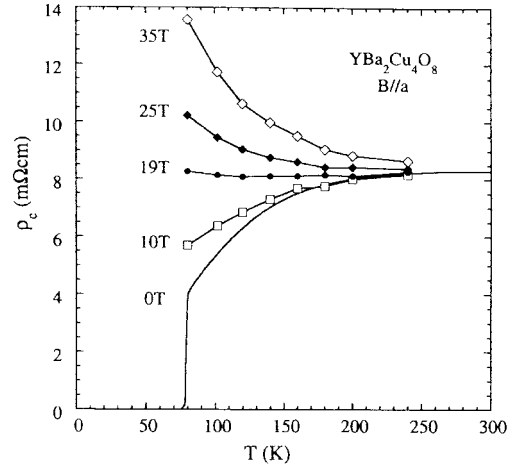


**Fig. 2.**  $\rho_c(T)$  curves for various fields  $\mathbf{H} \parallel a$ , taken from [7].

since the scaling dimension of time is fixed by

$$t \propto L^z \propto \xi^z.$$

The relaxation time  $\tau$  describes the rate at which the system relaxes to equilibrium.  $\tau$  diverges at the transition and the dynamic critical exponent  $z$  is defined as

$$\tau \propto \xi_\tau \propto \xi^z \propto |\epsilon|^{-z\nu}.$$

For  $H \neq 0$  the scaling expression for the conductivity reads as

$$\sigma(T, H) = \xi^{2-D+z} \mathcal{G}(\mathcal{Z}), \quad \mathcal{Z} = \frac{H(\xi^\pm)^2}{\Phi_0}. \quad (10)$$

Supposing then that there is a critical point at  $\mathcal{Z} = \mathcal{Z}_c$  with

$$2 - D + z = 0, \quad (11)$$

the curves  $\sigma$  versus  $H$  recorded at different temperatures  $T$  will cross at  $H = H_c$ , where  $\mathcal{Z} = \mathcal{Z}_c$ . The extension to anisotropic systems reads as

$$\sigma_{ii} = \frac{\xi_i \xi_\tau}{\xi_j \xi_k} \mathcal{G}(\mathcal{Z}), \quad (12)$$

with  $(i, j, k) \equiv (x, y, z)$  and  $\mathcal{Z}$  given by equation (7).

We are now prepared to analyze the resistivity data of Hussey *et al.* [7]. At  $H = 0$ , the material is supposed to undergo a continuous SN transition belonging to the 3D-XY universality class, and accordingly

$$\xi_{x,y,z} = \xi_{0,x,y,z} |\epsilon|^{-\nu}, \quad \xi_\tau \propto |\epsilon|^{-z\nu}, \quad \nu \approx 2/3. \quad (13)$$

If the transition occurs in finite fields, then  $\mathcal{Z} = \mathcal{Z}_c$ , and close to  $T_c = T_c(H = 0)$  the phase transition line is given by

$$H_{c,i} = \frac{\mathcal{Z}_c \Phi_0}{\xi_{0,j} \xi_{0,k}} |\epsilon|^{2\nu}, \quad (i, j, k) \equiv (x, y, z). \quad (14)$$

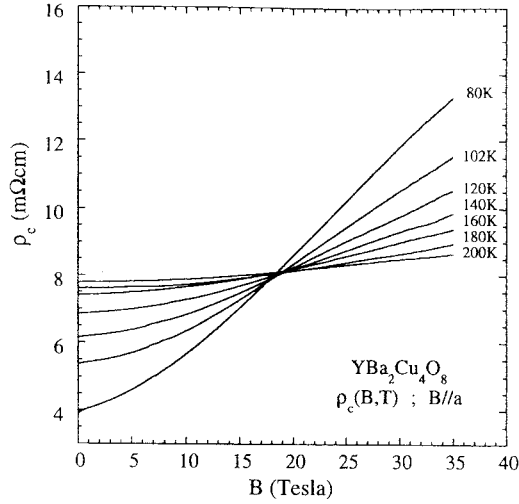


**Fig. 3.**  $\rho_c$  versus  $H$ ,  $\mathbf{H} \parallel a$  for various temperatures, taken from [7].

From Figure 1 it is seen that the resulting behavior for  $H_{c,z}$  (*i.e.*  $\mathbf{H} \parallel c$ ), namely

$$T_c(H) = T_c(H=0) \left(1 - 0.078H^{3/4}\right), \quad (15)$$

agrees remarkably well with the experimental data. Similarly, for  $H_{c,y}$  ( $\mathbf{H} \parallel a$ ) we obtain the estimate (using the two points  $T_c(H=0) = 80$  K,  $T_c(H=35 \text{ T}) = 65$  K measured by [7])

$$T_c(H) \approx T_c(H=0) \left(1 - 0.013H^{3/4}\right), \quad (16)$$

which has been included in the phase diagram shown in Figure 4. Combining equations (14–16), we obtain for the  $yz$ -anisotropy of the correlation lengths the estimate

$$\frac{\xi_y}{\xi_z} \approx \left(\frac{0.078}{0.013}\right)^{4/3} \approx 11, \quad (17)$$

which is close to the value obtained from magnetic torque measurements [13].

According to Figures 2 and 3, showing  $\rho_c$  vs. temperature for various fields ( $\mathbf{H} \parallel a$ ) as well as  $\rho_c$  vs.  $H$  ( $\mathbf{H} \parallel a$ ) for various temperatures between 80 K and 200 K, the behavior of the  $c$ -axis resistivity for a field oriented along the  $a$ -axis differs drastically from the ( $\mathbf{H} \parallel c$ ) data. Indeed, it is seen that in the normal state  $T_c < T < 200$  K for ( $\mathbf{H} \parallel a$ ) a NI transition occurs. In particular, all  $\rho_c(\mathbf{H} \parallel a)$  curves go through a single crossing point (Fig. 3) at

$$H_{cr} \approx 19 \text{ T}, \quad \rho_{c,cr} \approx 8 \text{ m}\Omega \text{ cm},$$

which is the value where  $\rho_c(T)$  becomes essentially temperature independent (Fig. 2). Nevertheless, there is still a transition into a superconducting regime beyond  $H_{cr} \approx 19$  T for  $\mathbf{H} \parallel a$  (*e.g.*  $T_c(35 \text{ T}) = 65$  K). One clearly observes in Figure 2 that at low magnetic fields ( $H < H_{cr} \approx 19$  T), as the temperature is reduced,  $\rho_c(T)$  shows a drop from

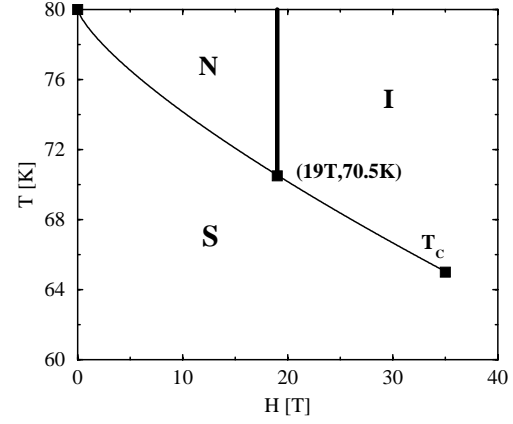


**Fig. 4.** Sketch of the  $T$ - $H$ -phase diagram, Y-124,  $\mathbf{H} \parallel a$ , deduced from the experimental data shown in Figures 2 and 3. The solid line corresponds to equation (16). S: Superconductor; I: Insulator; N: Normal conductor.

its normal state value  $\rho_c \approx 8$  m $\Omega$  cm. For  $H > H_{cr} \approx 19$  T and  $T > T_c(H)$ ,  $\rho_c$  raises with decreasing temperature, signalling the onset of insulating behavior. The resulting phase diagram, showing SN, SI and NI transitions as well as a multicritical point, where the superconducting, normal conducting and insulating phases can coexist, is drawn in Figure 4. On physical grounds one expects that the NI transition line will have a critical endpoint in the normal state, too.

The existence of the crossing point (critical field) in the bulk material ( $D = 3$ ) (Fig. 3) implies according to equation (11) that the dynamical critical exponent of the NI transition is  $z = 1$ . As a consequence, the scaling form of the conductivity (Eq. (12)) reduces for  $\mathbf{H} \parallel (a, b)$  to

$$\sigma_{zz} = \frac{\xi_{z0}\xi_{\tau 0}}{\xi_{x0}\xi_{y0}} \mathcal{G}(\mathcal{Z}_c) \text{ for } z = 1, D = 3, \quad (18)$$

where

$$\mathcal{Z}_c = \frac{\xi_z \xi_y H_c}{\Phi_0} \sqrt{\cos^2(\phi) + \left(\frac{\xi_x}{\xi_y}\right)^2 \sin^2(\phi)}. \quad (19)$$

Thus, curves  $\rho_c$  vs.  $H$  ( $\mathbf{H} \parallel a$ ), recorded at different temperatures  $T$ , exhibit a crossing point at  $H = H_{cr}$ , where  $\mathcal{Z} = \mathcal{Z}_c$ , in agreement with the experiment (Fig. 3). Moreover, if the data for  $H \parallel a$ , as shown in Figure 3, are replotted according to

$$\sigma_{zz} = \mathcal{F}(h/t^{2\nu}), \quad (20)$$

with  $h = |H - H_{cr}|/H_{cr}$  and  $t = |T - T_c(H_{cr})|/T_c(H_{cr})$ , they collapse, as shown in Figure 5, onto two branches (using  $T_c(H_{cr}) \approx 70.5$  K,  $H_{cr} \approx 19$  T and  $\nu \approx 2/3$ ).

Finally, close to the NI transition ( $\mathcal{Z} = \mathcal{Z}_c$ ) we obtain

$$\sigma_{zz} \approx \sigma_{zz}(\mathcal{Z}_c) + \left. \frac{\partial \sigma_{zz}}{\partial \mathcal{Z}} \right|_{\mathcal{Z}=\mathcal{Z}_c} (\mathcal{Z} - \mathcal{Z}_c), \quad (21)$$

where

$$\mathcal{Z} - \mathcal{Z}_c = (H - H_{cr}) \frac{\xi_z \xi_y}{\Phi_0} \sqrt{\cos^2 \phi + \left(\frac{\xi_x}{\xi_y}\right)^2 \sin^2 \phi}. \quad (22)$$

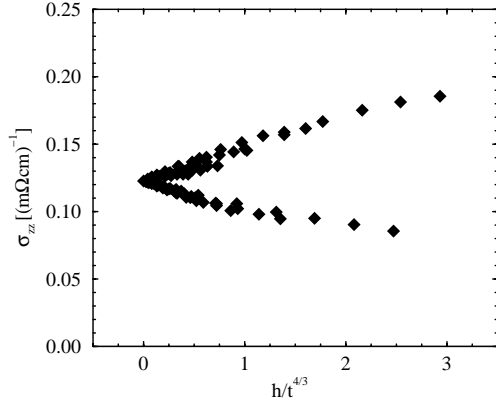


**Fig. 5.**  $\sigma_{zz}$  vs.  $h/t^{4/3}$  for the data shown in Figure 3. Upper branch:  $H < H_{cr}$ ; lower branch:  $H > H_{cr}$ .

Thus, provided that  $\xi_y \neq \xi_x$ , both, out-of-plane conductivity and resistivity will depend on the angle  $\phi$ , so that close to the multicritical point

$$\Delta\rho_{zz} = \frac{1}{\sigma_{zz} - \sigma_{zz}(Z_c)} = \left( \frac{\partial\sigma_{zz}}{\partial Z} \Big|_{Z=Z_c} (H - H_{cr}) \right) \times \frac{\xi_z \xi_y}{\Phi_0} \sqrt{\cos^2 \phi + \left( \frac{\xi_x}{\xi_y} \right)^2 \sin^2 \phi}^{-1}. \quad (23)$$

Figure 6 shows a fit of the Y-124 data to equation (23), this expression describes the experimental data very well, yielding  $\xi_x/\xi_y = 1.27$ , in fair agreement with a recent experimental estimate  $\xi_x/\xi_y \approx 1.6$  [14].

The value of the conductivity at the multicritical point ( $\rho_{c,cr} \approx 8 \text{ m}\Omega \text{ cm}$ ,  $\mathbf{H} \parallel a$ )

$$\sigma_{zz}(Z_c) = \frac{\xi_{z0}\xi_{\tau 0}}{\xi_{x0}\xi_{y0}} \mathcal{G}(Z_c) \approx 1/8 \text{ (m}\Omega \text{ cm)}^{-1} \quad (24)$$

puts a constraint for its occurrence for general magnetic field orientations. In particular, for  $H \parallel (z = c)$ , this value was not attained in the experiments considered here. For this reason there is no evidence for a NI-transition (see Fig. 1). Nevertheless, as function of the angle  $\delta$  a line of multicritical points, associated with a surface of SI-transitions, is expected to occur in the phase diagram  $(H, T, \delta)$  (see Fig. 4), as long as the constraint (24) is met with  $\delta$  decreasing from  $90^\circ$ .

To summarize, we have shown that the magnetic field and temperature dependence of the  $c$ -axis resistivity in  $\text{YBa}_2\text{Cu}_4\text{O}_8$ , recorded for various magnetic field orientations, can be understood in terms of the scaling theory of static and dynamic classical critical phenomena. For  $\mathbf{H} \parallel c$  we identified a SN transition, while for  $\mathbf{H} \parallel a$  we identified a magnetic field tuned NI-transition with the dynamical critical exponent  $z = 1$ , as well as a multicritical point, where superconducting, normal conducting and insulating phases can coexist. Moreover, for

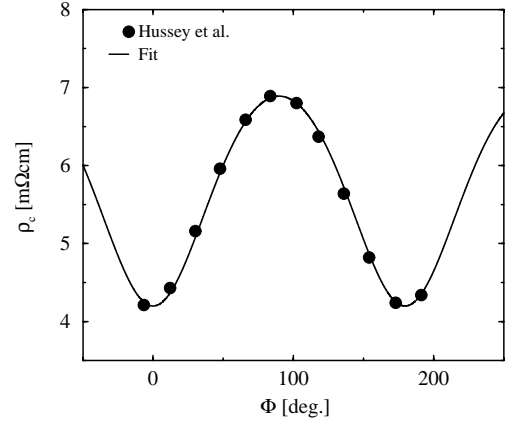


**Fig. 6.** Angular dependence of the  $c$ -axis resistance  $\rho_c$  recorded at  $T = 85 \text{ K}$  and field  $H = 15 \text{ T}$ . The field is rotated in the  $ab$ -plane. Experimental data (circles) are taken from [7], the solid line is a fit to expression (23), yielding  $\xi_x/\xi_y = 1.27$ .

general magnetic field orientations, we predicted a line of multicritical points provided that the critical resistivity  $\rho_{c,cr}$  is attainable.

We benefitted from discussions with H. Keller, J. Hofer and M. Willemin. Part of the work was supported by the Swiss National Science Foundation.

## References

1. T. Schneider, Acta Phys. Polon. A **91**, 203 (1997).
2. T. Schneider, J.M. Singer, Europhys. Lett. **40**, 79 (1997).
3. N. Marković, C. Christiansen, A.M. Goldman, Phys. Rev. Lett. **81**, 5217 (1998).
4. Y. Ando, G.S. Boebinger, A. Passner, T. Kimura, K. Kishio, Phys. Rev. Lett. **75**, 4662 (1995).
5. A. Malinowski, M.Z. Cieplak, A.S. van Stenbergen, J.A.A.J. Perenboom, K. Karpińska, M. Berkowski, S. Guha, P. Lindemfeld, Phys. Rev. Lett. **79**, 495 (1997).
6. G.A. Levin, T. Stein, C.C. Almasan, S.H. Han, D.A. Gajewski, M.B. Maple, Phys. Rev. Lett. **80**, 841 (1998).
7. N.E. Hussey, M. Kibune, N. Nakagawa, N. Miura, Y. Iye, H. Takagi, S. Adachi, K. Tanabe, Phys. Rev. Lett. **80**, 2909 (1998).
8. P.C. Hohenberg, B.I. Halperin, Rev. Mod. Phys. **49**, 435 (1977).
9. T. Schneider, J. Hofer, M. Willemin, J.M. Singer, H. Keller, Eur. Phys. J. B **3**, 413 (1998).
10. T. Schneider, J.M. Singer, to be published in Physica C (1999); cond-mat/9812082.
11. M. Hubbard, M.B. Salamon, B.W. Veal, Physica C **259**, 309 (1996).
12. J. Hofer, T. Schneider, J.M. Singer, M. Willemin, C. Rossel, H. Keller, submitted for publication to Phys. Rev. B (1998).
13. D. Zech, C. Rossel, L. Lesne, H. Keller, S.L. Lee, J. Karpinski, Phys. Rev. B **54**, 12535 (1996).
14. D.N. Basov *et al.*, Phys. Rev. Lett. **74**, 598 (1995).